9

Research Article

Mohammed Y. Fattah*, Hussein H. Hussein, Mohammed F. Aswad and Reham E. Hamdi

Studying the lateral displacement of retaining wall supporting sandy soil under dynamic loads

https://doi.org/10.1515/eng-2022-0553 received September 23, 2023; accepted October 30, 2023

Abstract: When Rankine or Coulomb theories are used to design a retaining wall, it is accepted that the retaining wall will experience a lateral displacement. By allowing the wall to move laterally, the earth pressure decreases on the active side of the wall and wall and earth pressure increases on the passive side, and therefore, more economical walls can be obtained when the lateral displacement is allowed. This lateral displacement is usually not calculated when designing a retaining wall. An experimental investigation is carried out to study the lateral displacement of a retaining wall subjected to dynamic loads with different load amplitude vibration, absolute frequencies, backfill sand relative densities, and different distances between the retaining wall and the loading source. The objectives of this study are to trace the lateral displacement of retaining wall under dynamic loads other than earthquakes such as the traffic load caused by trucks or railroads by direct measurement of displacements. The model footing used in this study is square. On a cohesionless soil, the tests were carried out using a dynamic load. The studied variables were as follows: three load amplitudes (0.25, 0.5, and 1 ton), three vibration frequencies (0.5, 1, and 2 Hz), two relative densities of sandy soil (30% loose sand and 70% dense sand), and three different distances between the foundation and the retaining wall. Observations show that the lateral displacement increased by increasing the load amplitude and decreased by increasing the distance between the foundation and the retaining wall. There is insignificant consequence of frequency on the cumulative lateral

displacement. The lateral displacement decreased by increasing the density of sandy soil.

Keywords: retaining wall, dynamic, lateral displacement, cohesionless soil, displacement sensors

1 Introduction

Retaining wall system is one of the most significant civil engineering structures developed to provide lateral support of soil and is broadly utilized in highway walls, mines, underground structures, military defense, and so on. Retaining systems consist mainly of a retaining wall and backfill soil; the engineering essence of retaining wall is to keep the retained soil in certain shape and prevent it from falling (stability), or to restrain the deformation of the wall and the backfill to maintain its service function (serviceability). To estimate the stability of these structures, an exact estimation of the lateral earth pressure is significant.

The issue of assessing seismically initiated lateral earth pressures on retaining structures has been first tended to during the 1920s in spearheading examination carried out in Japan Okabe [1], Mononobe and Matsuo [2]. Since then, this problem has received periodic attention from the research community (e.g., Seed and Whitman [3]; Nazarian and Hadjian [4]; Prakash [5]; Raheem and Fattah [6]; and Al-Juari et al. [7]); however, it had relatively little impact on the design engineering practice until relatively recently.

According to Zhang et al. [8], the seismic coefficient and the method of wall movement influence the height at which P_E is applied. For rotating wall movement modes, the size of max has a big impact on height. The resulting force is discovered to act at a height of 0.3 to 0.4 H in each example.

The conductance of lateral displacement on sandy soil subjected to dynamic loads was treated by several researchers who demonstrated the soil's response to a dynamic load using a theoretical method using finite element analysis.

Akhlaghi and Nakhodchi [9] investigated the dynamic response of cantilever retaining walls to seismic loads. They explore how the mechanical characteristics of the

e-mail: myf_1968@yahoo.com

Hussein H. Hussein: Civil Engineering Department, University of Warith Al-Anbiyaa, Karbala, Iraq, e-mail: h.hussein@uowa.edu.iq.

Mohammed F. Aswad: Civil Engineering Department, University of Technology, Baghdad, Iraq,

e-mail: mohammed.f.aswad@uotechnology.edu.iq

Reham E. Hamdi: Civil Engineering Department, University of Technology, Baghdad, Iraq, e-mail: rehamemad9568@gmail.com

^{*} Corresponding author: Mohammed Y. Fattah, Civil Engineering Department, University of Technology, Baghdad, Iraq,

soil and wall affect the dynamic behavior of a cantilever retaining wall using the Plaxis software. Additionally, the effects of the source vibration's amplitude and frequency on the response of the wall have been investigated and discussed. The findings show that wall displacement increases with increasing soil density and harmonic load amplitude, whereas wall dynamic response reduces with increasing soil values for friction angle, cohesion, elasticity, and damping.

Ling et al. [10] conducted parametric research on the behavior of reinforced soil retaining walls under earth-quake loading by finite element analysis. They conducted a general analysis of the lateral displacement of retaining structures subjected to dynamic stresses. The study's findings showed that the top of the wall had the most lateral displacement and that the amplitude of harmonic loads increased, while the dynamic response of the wall decreased as friction angle, cohesion, elasticity, and soil damping values increased.

Chowdhury and Dasgupta [11] developed a comprehensive analytical approach based on modal analysis that considers the impact of the wall's temporal period, a factor that has largely been disregarded by other studies. Thus, the work was an effort to reconsider this age-old subject and find answers to many of the unresolved problems listed earlier. Almost every form of soil and loading condition that might be present in a real-world design is also addressed, including liquefaction, whose effects on the wall undoubtedly require further study.

Salman et al. [12] assumed that wall displacement increases as the soil's Poisson's ratio grows in value. The retaining wall's behavior is influenced by the different Poisson's ratio estimations of the foundation soil.

Jose et al. [13] conducted an experimental investigation using retaining wall lateral displacement. When the Rankine or Coulomb theories are used to construct a retaining wall, it is already realistic to expect lateral displacement. This alternative is not frequently considered when designing a retaining wall. This study describes a method for estimating the retaining wall lateral displacement in addition to the soil's friction angle, cohesion, elasticity, and damping.

The impact of earthquake features on the long-term displacement of a cantilever retaining wall was examined by Bakr and Ahmad [14]. The study mainly focused on assessing the impact of earthquake characteristics and seismic ground pressure on permanent seismic displacement. The results revealed that the Newmark block sliding approach overestimates permanent seismic displacement. The most important scenario, causing maximum permanent displacement, is when the ground motion is of maximum capacity but has minimum frequency content. Earth seismic pressure has a low impact on permanent displacement.

Bakr and Ahmad [15] provided a novel finite element model-based analysis and development of a link between seismic active and passive earth pressure and stiff retaining wall movement. For soil modeling, a hardening soil with small strain model with Rayleigh damping has been used. The finite element model was validated using centrifuge test results that were already accessible in the literature. Unique design charts illustrating the relationship between seismic ground pressure and wall movement have been proposed. The seismic active earth pressure is found to be independent of the seismic input motion and hence does not depend on wall movement during an earthquake, whereas the seismic passive earth pressure is greatly affected by it. It is abundantly obvious from a comparison of the study's findings with those obtained using the Mononobe-Okabe and pseudo-dynamic approaches that the latter overestimates seismic ground pressure. The suggested design charts and other findings offer the design engineers a crucial hint.

The objective of this study is to trace the lateral displacement of retaining wall under dynamic loads other than earthquakes such as the traffic load caused by trucks or railroads by direct measurement of displacements.

2 Laboratory work

2.1 Soil properties

The soil used in this study is a natural cohesionless soil (sand) imported from Karbala city, Iraq. The entire sample was sieved using sieve No. 10 (2.0 mm), and then, the sieved sample was subjected to conventional tests to find out the soil's physical characteristics. According to the Unified Soil Classification System, the soil is categorized as SP-SM soil. In Table 1, a summary of the test results is provided along with each test's criteria. The size distribution of the soil grains used is shown in Figure 1.

2.2 Steel container

A steel container with plan dimensions of 1,500 mm in length, 900 mm in width, and 1,000 mm in height was used for the experiments. The container was composed entirely of 5 mm thick steel plate. The container was constructed from five carefully welded sections, one of which served as the base and the other four as its four sides. The angles at the borders of the long sides served as external

Table 1: Physical parameters of the sand used in the experiments

Parameter	Results	Specification
Specific gravity (<i>G</i> _s)	2.65	ASTM D854 [16]
Gravel %, >4.75 mm	0	ASTM D422 [17]
Sand %, 0.075–4.75 mm Clay and silt %, <0.075 mm	96 4	ASTM D422 [17] ASTM D422 [17]
D_{60} , mm	0.5	ASTM D422 [17] ASTM D422 [17]
D ₃₀ , mm	0.3	ASTM D422 [17]
D ₁₀ , mm	0.17	ASTM D422 [17]
Coefficient of uniformity, Cu	2.94	ASTM D422 [17]
Coefficient of curvature, Cc	1.06	ASTM D422 [17]
Minimum dry unit weight, kNm ³	15.5	ASTM D4253 [18]
Maximum dry unit weight, kN/m ³	17.2	ASTM D 4254 [19]
Maximum void ratio, e _{max}	0.68	_
Minimum void ratio, e_{min}	0.51	_
Soil classification	SP-SM	ASTM D2487 [20]

bracing. Three channels of 50 mm web and 25 mm flange were used to externally strengthen the base.

2.3 Load application device

In order to investigate the experimental distribution of lateral stress behind the wall due to the dynamic load, the vibration loading equipment was developed and constructed in the laboratories of the University of Technology, specifically in the Soil Mechanics Laboratory. The device was designed with a load capacity of 60 kN. This load capacity

was achieved using hydraulic compressor system [21], as shown in Figure 2.

The following components comprise the load application devices:

1. loading frame made of steel, 2. electrical hydraulic system, 3. load spreader plate, 4. instruments for measuring settlement, 5. system for data collection and logging, and 6. container made of steel (1,500 \times 900 \times 1.000 mm).

2.4 Steel loading frame

A steel frame was designed and built to support and ensure the verticality of the hydraulic jack used to apply the centrally concentrated load. The steel frame is made up mostly of four columns and four beams. Each column and each beam are composed of steel and have a square cross-section area of 100 mm by 100 mm and a thickness of 4 mm. The steel frame's measurements (length × width × height) are 1.700 mm × 700 mm × 1.700 mm.

2.5 Electrical hydraulic system

A hydraulic steel tank with a capacity of 70 L is included in the system. The tank has two holes: the upper one for filling the oil and the bottom one for discharge. The tank

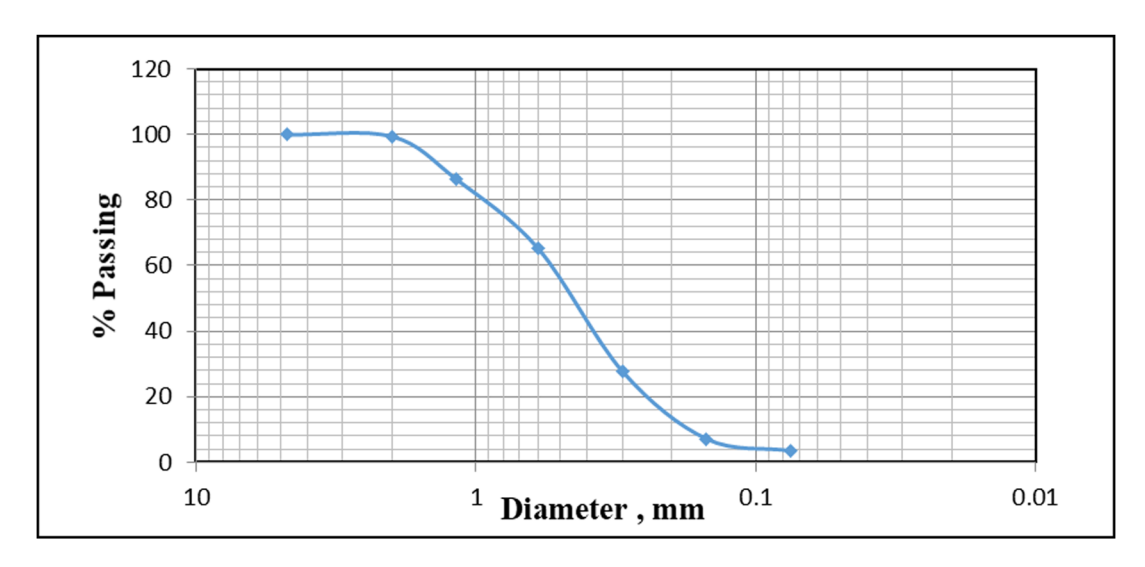


Figure 1: Grain size distribution for the used soil.

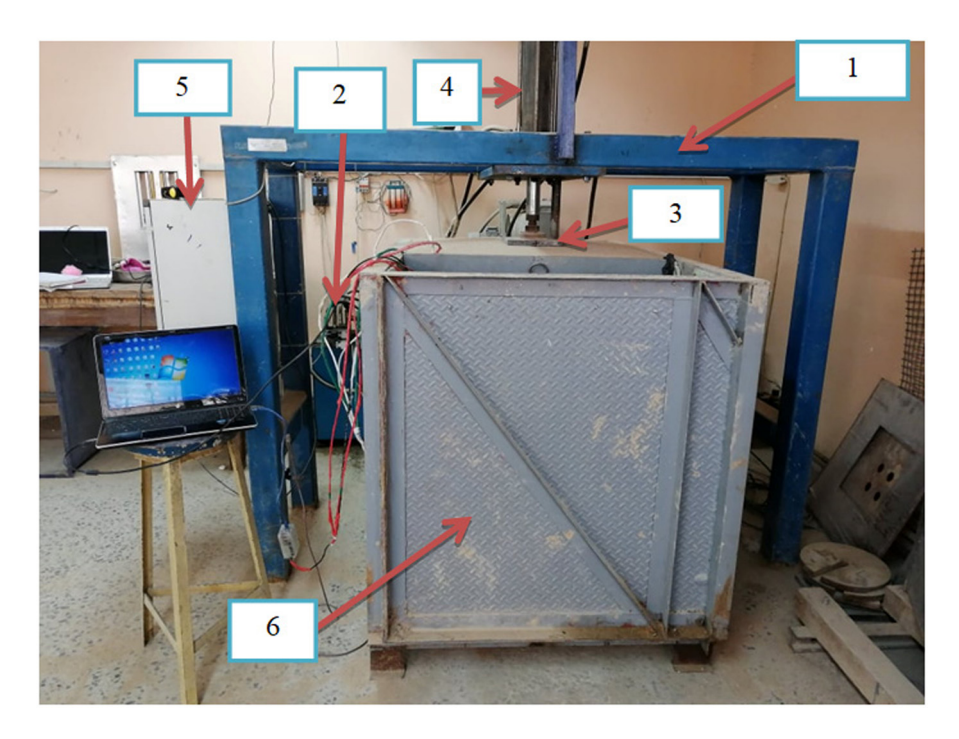


Figure 2: Vibratory loading device. 1. loading frame made of steel, 2. electrical hydraulic system, 3. load spreader plate, 4. instruments for measuring settlement, 5. system for data collection and logging, and 6. container made of steel.

contains a gear-type hydraulic pump with a set geometrical volume that produces a discharge of around 12 L/min at a maximum pressure of 150 bars.

is used to view input and output data using simplified ladder logic.

2.6 Loading spreader plate

For the application of the dynamic load, a square balance ($200 \text{ mm} \times 200 \text{ mm}$) made of solid steel that was 20 mm thick was utilized. The dynamic load that has been imposed on this footing corresponds to the traffic load on railways or vehicles.

2.7 Data acquisition and logging structure

The data collection system is used to detect and sense the displacement that occurs throughout the testing, allowing the tester to obtain a large number of readings in a short period of time. It is also used to select the specific frequency utilized in the test. The data acquisition system is made up of a programmable logic controller (PLC), which is a high-tech processing unit and can be defined as a digital computer utilized for electro-mechanical automation processes. Data are digitally analyzed by this type of equipment. A PLC device with an LCD touch-screen display

2.8 Gravity wall model

The gravity wall was made of steel and had a width of 16 mm at the top and 60 mm at the bottom, a height of 700 mm, and a length of 850 mm. These dimensions were determined in accordance with Bowels' [22] criteria, as shown in Figure 3. The steel retaining wall is depicted in Figure 4.

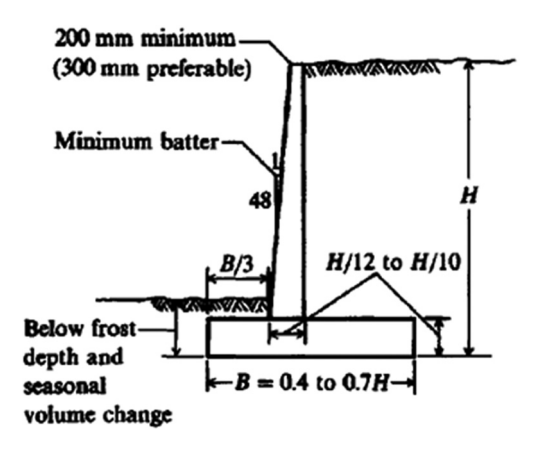


Figure 3: Design specifications for a cantilever retaining wall [22].



Figure 4: Manufactured retaining wall.

2.9 Instrumentation

A time-off-light sensor is employed. It is a laser distance sensor using a 940 nm laser. It can accurately measure distances up to 1,250 mm. The sensor can report distances of up to 2 m (6.6 ft) with a precision of 1 mm, although its actual range and accuracy (noise) are strongly dependent on ambient circumstances, target features such as reflectance and size, as well as sensor design. The sensor's accuracy is specified to be between 3 and 10% under ideal conditions. The UNO board used, to begin with, hardware and coding. Soil arrangement, retaining wall, and laser displacement placement in the box are exhibited in Figures 4-6. A displacement transducer that was integrated into the hydraulic jack body was used to measure vertical settlements. This settlement indicates the average settlement for the footing.

A total of 54 model experiments were carried out on sandy soil using two different relative densities: 30 and 70%, which correspond to loose and dense sand, respectively. Following the completion of the sandy soil preparation, the top surface was leveled to get the closest possible flat surface. The model's top surface was then used to acquire the footing. After the planning of footing superficially layer of sand, the dynamic load was applied all through a foreordained arrangement. The use of dynamic load proceeds up to 10,000 cycles. The distance-measuring instruments were placed in front of the wall, two of them on the right and left and at a height of 200 mm and the middle at a height of 300 mm from the height of the box.

The load wave was half sine wave (only positive), it was examined by taking 20 readings/s under the load lever, ensuring that only the positive portion of the load frequency is applied when a broader load is applied. This ensures that the device applies a pocket dynamic load at various frequencies. The way to represent this load is with a frequency, rotary, or rail track. These machines' loading patterns are all more or less sinusoidal and can be admired as a sine wave.

$$F(t) = a \sin \omega t, \tag{1}$$

where a is the amplitude dynamic load and ω is the frequency.

When compared to the typical frequency of the railroad track, which is around 8-10 Hz, this frequency is regarded as low. However, this frequency was connected to the hydraulic loading system's pressure and flow capacity. The frequency being employed falls within the range of reciprocating machine frequencies.



Figure 5: Placing the laser displacement in front of wall in the box.



Figure 6: Model footing and retaining wall during the test.

3 Results of the model test subjected to dynamic load

3.1 Influence of dynamic loads on lateral displacement

The relationship between the lateral displacement and the number of cycles for different load amplitudes for particular models is shown in Figures 7–12. The data presented obviously show that the amount of lateral displacement grew as the load amplitude rose. It can be shown that the accumulated lateral displacement is only slightly impacted

by recurrence. By increasing the relative density, the values of lateral displacement decreased. Likewise, by increasing the distance between the foundation and the retaining wall, the values of lateral displacement were reduced.

3.1.1 1. Lateral displacement at depth 200 mm from the box top level (active side)

Figures 7–12 illustrate the result of lateral displacement versus number of cycle on loose and dense sand of relative densities $D_{\rm r}$ = 30% and $D_{\rm r}$ = 70% by laser displacement

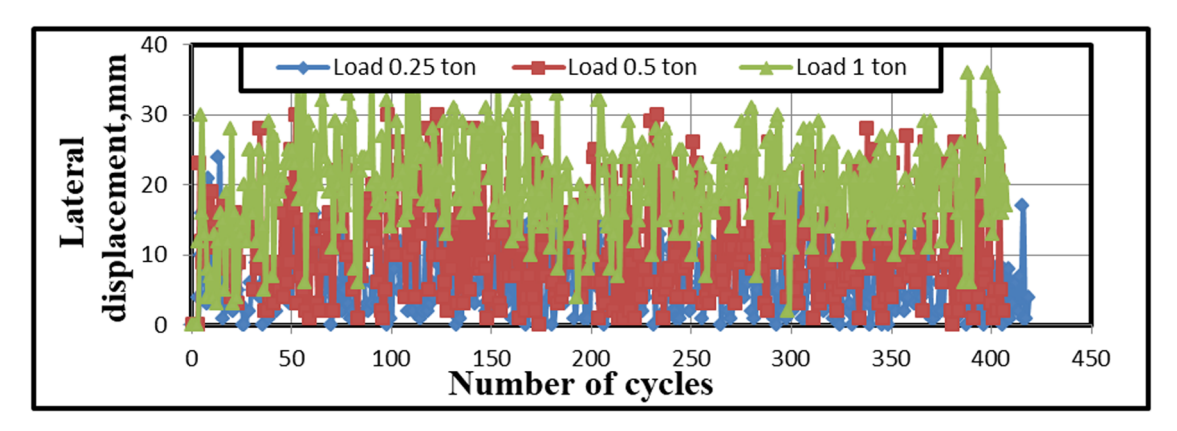


Figure 7: Lateral displacements vs cycle number for various load amplitudes with relative density D_r = 30% and frequency 0.5 Hz when the load is applied at a distance equal to 0.2 H.

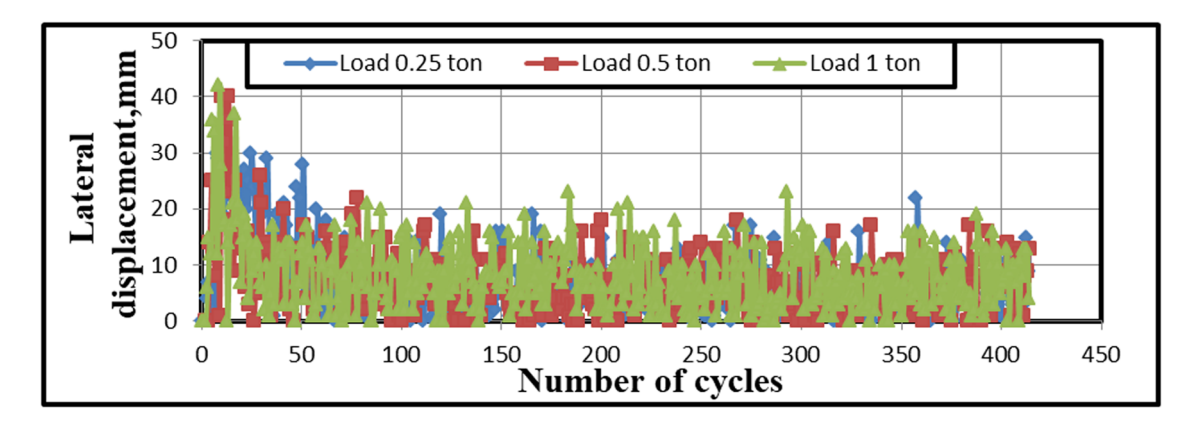


Figure 8: Lateral displacements vs cycle number for various load amplitudes with relative density D_r = 70% and frequency 0.5 Hz when the load is applied at a distance equal to 0.2 H.

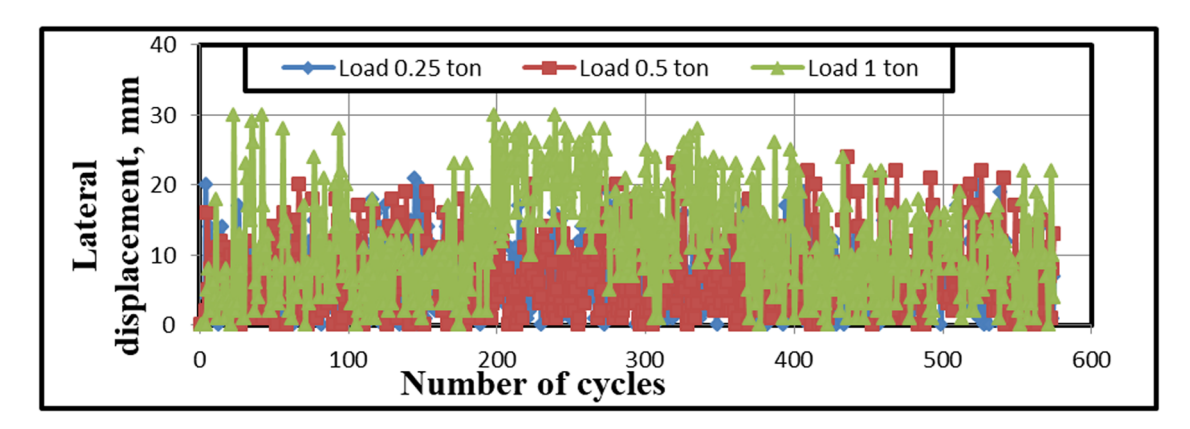


Figure 9: Lateral displacements vs cycle number for various load amplitudes with relative density $D_r = 30\%$ and frequency 1 Hz when the load is applied at a distance equal to 0.2 H.

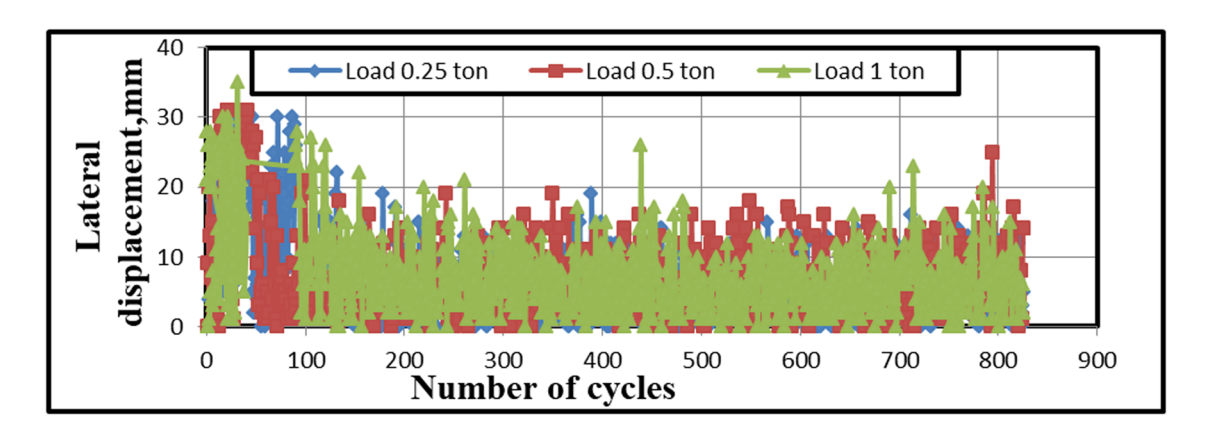


Figure 10: Lateral displacements vs cycle number for various load amplitudes with relative density $D_r = 70\%$ and frequency 1 Hz when the load is applied at a distance equal to 0.2 H.

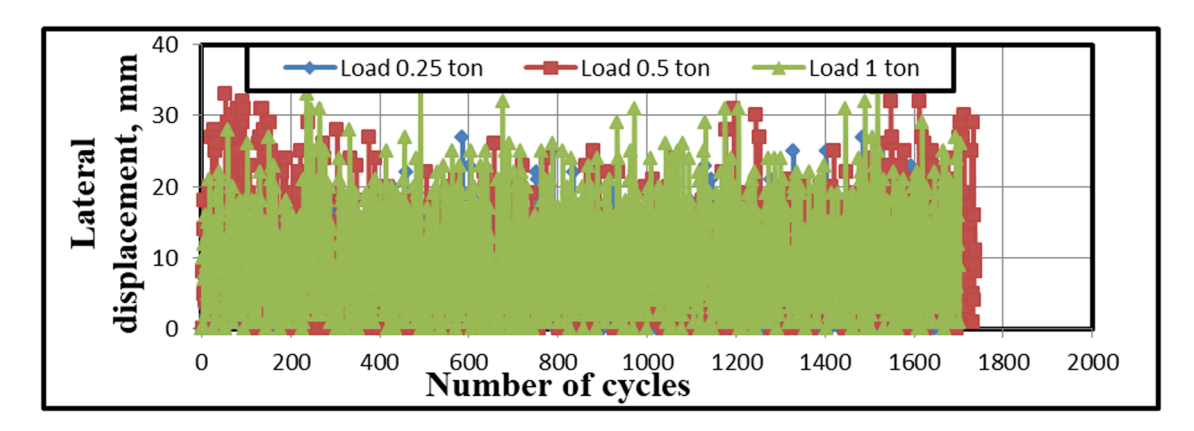


Figure 11: Lateral displacements vs cycle number for various load amplitudes with relative density D_r = 30% and frequency 2 Hz when the load is applied at a distance equal to 0.2 H.

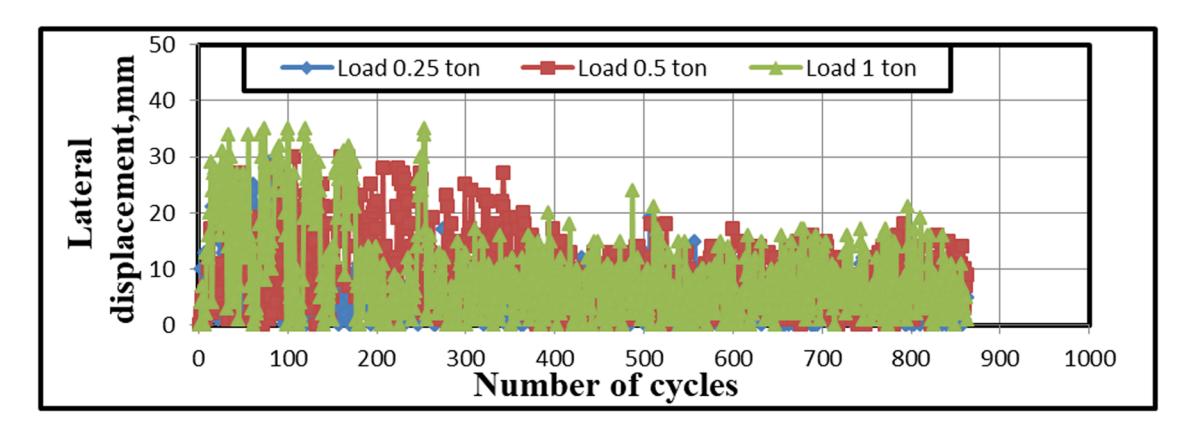


Figure 12: Lateral displacements vs cycle number for various load amplitudes with relative density $D_r = 70\%$ and frequency 2 Hz when the load is applied at a distance equal to 0.2 H.

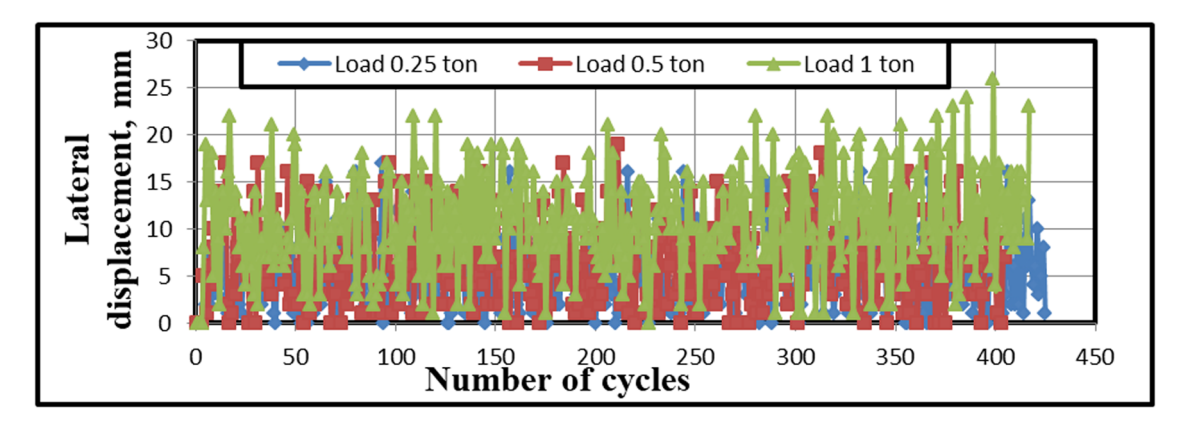


Figure 13: Lateral displacements vs cycle number for various load amplitudes with relative density $D_r = 30\%$ and frequency 0.5 Hz when the load is applied at a distance equal to 0.2 H.

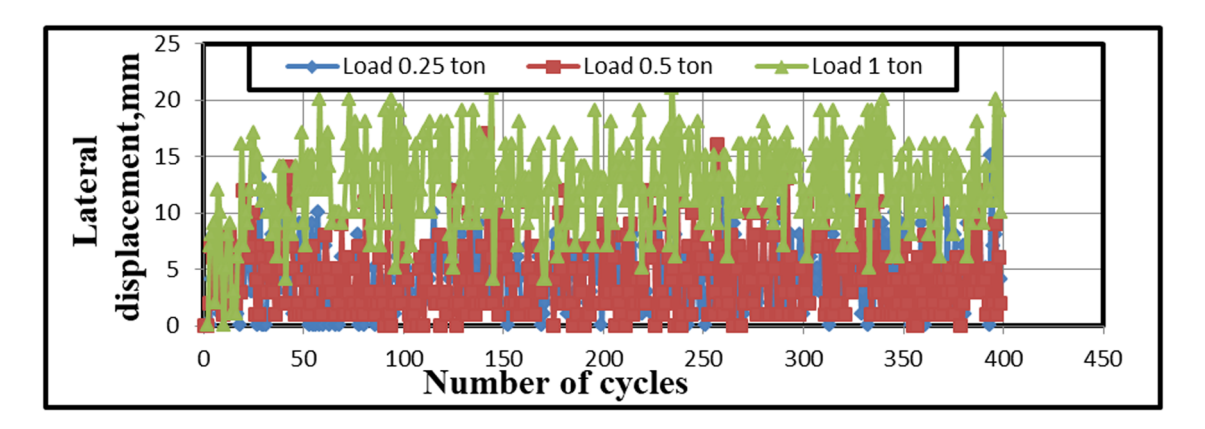


Figure 14: Lateral displacements vs cycle number for various load amplitudes with relative density D_r = 70% and frequency 0.5 Hz when the load is applied at a distance equal to 0.2 H.

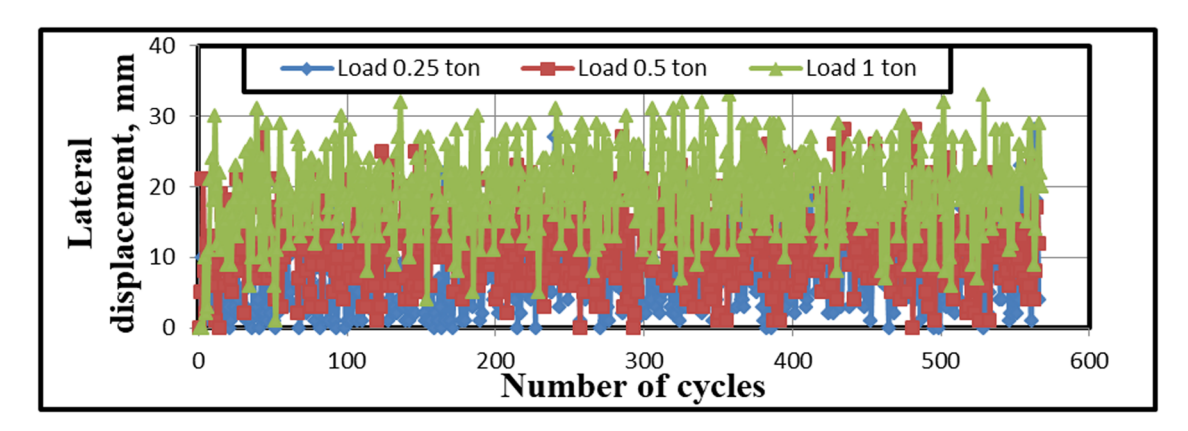


Figure 15: Lateral displacements vs cycle number for various load amplitudes with relative density $D_r = 30\%$ and frequency 1 Hz when the load is applied at a distance equal to 0.2 H.

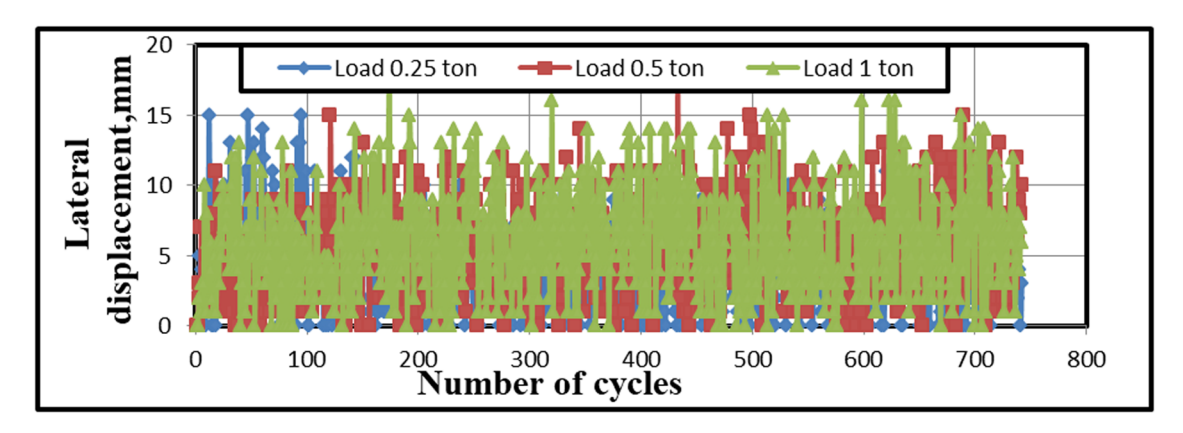


Figure 16: Lateral displacements vs cycle number for various load amplitudes with relative density $D_r = 70\%$ and frequency 1 Hz when the load is applied at a distance equal to 0.2 H.

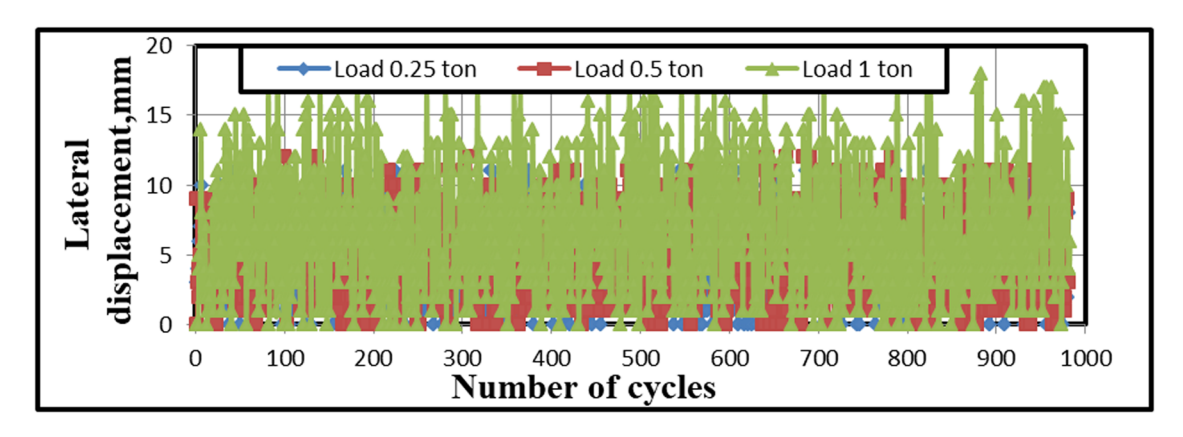


Figure 17: Lateral displacements vs cycle number for various load amplitudes with relative density $D_r = 30\%$ and frequency 2 Hz when the load is applied at a distance equal to 0.2 H.

placed at depth 200 mm of the box on the left points in front of retaining wall.

3.1.2 2. Lateral displacement at depth 200 mm from the box top level (passive side)

Figures 13–18 illustrate the results of lateral displacement versus number of cycles for model walls on loose and

dense sand of relative densities $D_{\rm r} = 30\%$ and $D_{\rm r} = 70\%$ measured by laser displacement placed at depth 200 mm of the box on the right point in front of the retaining wall.

The values of the maximum lateral displacement at depth 200 mm at the right and left points of the box in front of the wall are shown in Tables 2 and 3 for the two relative densities of 30 and 70%, respectively.

Tables 4 and 5 condense the values of the maximum lateral displacement at depth 300 mm at the middle point

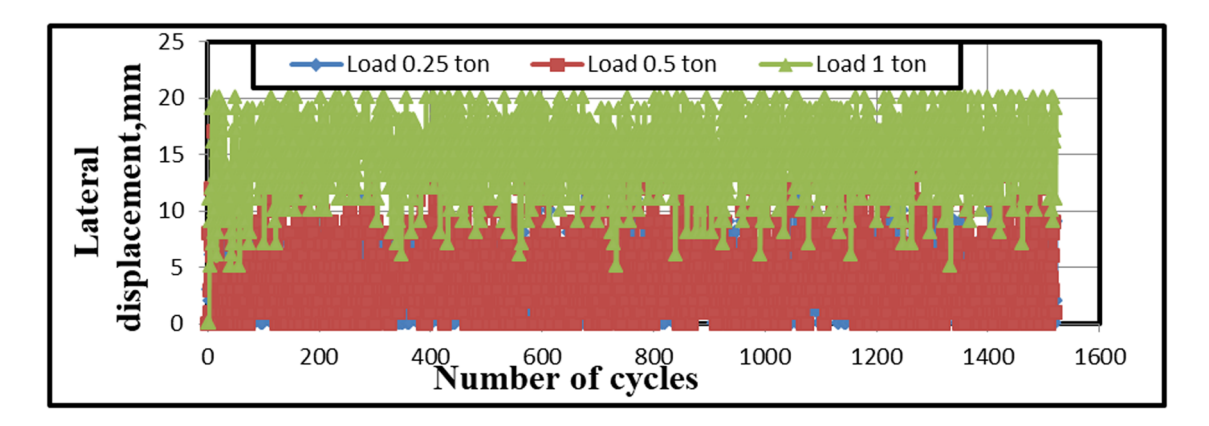


Figure 18: Lateral displacements vs cycle number for various load amplitudes with relative density $D_r = 70\%$ and frequency 2 Hz when the load is applied at a distance equal to 0.2 H.

Table 2: Lateral displacements versus load relationship for $D_r = 30\%$ and different frequencies

Load (ton)	Lateral displacements									
	0.5 Hz			1 Hz			2 Hz			
	0.2 H	0.3 H	0.4 H	0.2 H	0.3 H	0.4 H	0.2 H	0.3 H	0.4 H	
0.25	5.85	5.53	4.1	7.25	4.96	4.87	5.88	5.57	5.3	
0.5	9.3	8.03	5	9.55	7.69	5.79	7.2	6.75	6.39	
1	15.35	11.03	8.1	15.4	8.69	7.02	9.03	8.15	7.79	

Table 3: Lateral displacements versus load relationship for $D_r = 70\%$ and different frequencies

Load (ton)	Lateral displacements									
	0.5 Hz			1 Hz			2 Hz			
	0.2 H	0.3 H	0.4 H	0.2 H	0.3 H	0.4 H	0.2 H	0.3 H	0.4 H	
0.25	5.3	4.56	3.71	5.52	4.81	4.6	4.74	4.39	4.15	
0.5	5.7	5.01	4.6	6.93	6.1	5.4	6.19	6	4.86	
1	10.73	10.3	9.34	11.18	11.06	7	11.7	7.85	6.73	

Table 4: Lateral displacements versus load relationship for $D_r = 30\%$ and different frequencies

Load (ton)	Lateral displacements								
	0.5 Hz			1 Hz			2 Hz		
	0.2 H	0.3 H	0.4 H	0.2 H	0.3 H	0.4 H	0.2 H	0.3 H	0.4 H
0.25	2.4	2.01	2	2.32	2.11	1.78	2.5	2.1	1.8
0.5 1	3.08 7.34	2.9 4.5	2.7 3	4.3 4.8	3.05 3.68	2.2 2.8	3.7 6.4	2.67 3.98	2.06 3.75

Table 5: Lateral displacements versus load relationship for $D_r = 70\%$ and different frequencies

Load (ton)		Lateral displacements								
	0.5 Hz			1 Hz			2 Hz			
	0.2 H	0.3 H	0.4 H	0.2 H	0.3 H	0.4 H	0.2 H	0.3 H	0.4 H	
0.25	2.03	1.92	1.8	2	1.74	1.7	2.39	1.74	1.55	
0.5 1	2.29 6.18	2.24 3.08	2.11 2.7	2.5 4.17	2.37 2.59	2.18 2.35	3.5 4.65	2.26 3.9	1.9 2.91	

of the box in front of the wall for the two relative densities of 30 and 70%, respectively.

The lateral displacement caused by the active thrust on the wall will rise as the dynamic load amplitude increases, and this will be accompanied by a vertical displacement (settlement) of the backfill soil. The lateral active earth pressure on the wall, and thus, the lateral displacement will decrease as the relative density of the backfill soil rises; this, in turn, reduces soil settlement.

From figures and tables, it can be noted that the maximum lateral displacement happened at the greatest load amplitude and when the distance between foundation load and retaining wall is 0.2 H. The maximum lateral displacement measured by three laser displacements placed before the retaining wall revealed that the greatest displacement happened at a depth 200 mm from the top of the retaining wall. This was also concluded by Hoe et al. [23] where they used finite element analysis to investigate the behavior of

reinforced soil retaining walls under seismic loads. It was concluded that the maximum lateral displacement occurred at the top of the wall.

By referring to the aforementioned tables, it is observed that the values of lateral displacement are gradually increased by increasing the load when fixing other variables in these tables. For example, at a density of 30%, frequency of 0.5 Hz, and distance between the foundation and retaining wall of 0.2H, the lateral displacements under the load amplitudes of 0.5 ton and load of 1 ton are greater than the lateral displacement under the load amplitude of 0.25 ton in the rate of 37.1 and 61.9%, respectively. Also, at a density of 70%, frequency of 0.5 Hz, and distance between the foundation and retaining wall of 0.2H, the lateral displacements under load amplitudes of 0.5 ton and load of 1 ton are greater than the lateral displacement under load amplitude of 0.25 ton in the rate of 7.5 and 50.6%, respectively. According to the figures and tables, there is a slight rise in the induced lateral displacement when the load

amplitude is increased from 0.25 to 0.5 ton, but it is greater when the load amplitude is increased to 1 ton.

This was also observed by Bakr and Ahmad [14], who showed that the most important scenario, causing the maximum permanent displacement, is when the ground motion is of maximum capacity but has minimum frequency content. Earth seismic pressure has a low impact on permanent displacement.

4 Conclusions

The following conclusions could be drawn based on the results of the model experiments carried out on the various elements to assess the impact of the dynamic load on the lateral displacement of cohesionless backfill soil behind the retaining wall under dynamic load:

- 1. The lateral displacement rose as the load amplitude grew and reduced as the foundation's distance from the retaining wall increased.
- 2. There is a little impact of load frequency on the combined lateral displacement.
- 3. By raising the relative density of the soil of the backfill, the lateral displacement was reduced.

Funding information: Authors declare that the manuscript was done depending on the personal effort of the author, and there is no funding effort from any side or organization.

Conflict of interest: The authors state no conflict of interest.

Data availability statement: Most datasets generated and analyzed in this study are comprised in this submitted manuscript. The other datasets are available on a reasonable request from the corresponding author with the attached information.

References

- Okabe S. General theory of earth pressure. J Jpn Soc Civ Eng. 1926;12:1.
- [2] Mononobe N, Matsuo H. On the determination of earth pressure during earthquakes. Proc World Engr Conference. Vol. 9; 1929. p. 176.
- [3] Seed HB, Whitman RV. Design of earth retaining structures for dynamic loads. ASCE Specialty Conference, Lateral Stresses in the Ground and Design of Earth Retaining Structures. Ithaca, NY, USA: Cornell Univ; 1970. p. 103–47.
- [4] Nazarian HN, Hadjian AH. Earthquake induced lateral soil pressures on structures. J Geotech Eng Div ASCE. 1979;105(GT9):1049–66.

- [5] Prakash S. Dynamic earth pressures. State of the art report. Int Conf Recent Adv Geotech Earthquake Eng Soil Dyn. 1981. p. 993–1020.
- [6] Raheem AM, Fattah MY. Analysis of retaining wall subjected to earthquake loading. J Kirkuk Univ – Sci Stud. 2008;3(1):1–20.
- [7] Al-Juaria KAK, Fattah MY, Khattaba SIA, Al-Shamam MK. Experimental and numerical modeling of moving retaining wall in expansive soil. Geomech Geoeng. 2019. doi: 10.1080/17486025. 2019.1645363.
- [8] Zhang JM, Shamoto Y, Tokimatsu K. Seismic earth pressure theory for retaining walls under any lateral displacement. Soils Found. 1998;38(2):143–63.
- [9] Akhlaghi T, Nakhodchi A. Investigation of dynamic response of cantilever retaining walls using FEM. 16th International Conference on Soil Mechanics and Geotechnical Engineering. Vol. 1, No. 5. Osaka, Japan; 2005. p. 877–80.
- [10] Ling HI, Mohri Y, Leshchinsky D, Burke C, Matsushima K, Liu H. Large-scale shaking table tests on modular-block reinforced soil retaining walls. J Geotech Geoenviron Eng ASCE. 2005;131(4):465–76.
- [11] Chowdhury I, Dasgupta SP. An analytical solution to seismic response of a cantilever retaining wall with generalized backfilled soil. Electron J Geotech Eng. 2011;16:296–324 (Bund. C).
- [12] Salman FA, Fattah MY, Sabre DK. Long term behavior of a retaining wall resting on clayey soil. Int J Phys Sci. 2011;6(4):730–45.
- [13] José M, Nicolás S, Jesús Q. Lateral displacement of retaining walls. J Geol Resour Eng. 2016;6(16):251–6.
- [14] Bakr J, Ahmad SM. Effect of earthquake characteristics on permanent displacement of a cantilever retaining wall. In: Cardoso AS, Borges JL, Costa PA, Gomes AT, Marques JC, Vierira CS, editors. Numerical methods in geotechnical engineering IX. Taylor & Francis Group; 2018. ISBN 978-1-138-33198-3.
- [15] Bakr J, Ahmad SM. A finite element performance-based approach to correlate movement of a rigid retaining wall with seismic earth pressure. Soil Dyn Earthq Eng. 2018;114:460–79.
- [16] American Society of Testing and Materials (ASTM). Standard test method for specific gravity. ASTM D 854. West Conshohocken, PA, USA; 2010.
- [17] American Society of Testing and Materials (ASTM). Standard test method for particle size analysis of soils. ASTM D422-10. West Conshohocken, PA, USA; 2010.
- [18] American Society of Testing and Materials (ASTM). Standard test method for maximum index density and unit weight of soils using a vibratory table. ASTM D425300. West Conshohocken, PA, USA; 2006.
- [19] American Society of Testing and Materials (ASTM). Standard test method for minimum index density and unit weight of soils and calculation of relative density. ASTM D4254-00. West Conshohocken, PA, USA; 2006.
- [20] American Society of Testing and Materials (ASTM). Standard practice for classification of soils for engineering purposes (united soil classification system). ASTM D2487. West Conshohocken, PA, USA; 2006.
- [21] Fattah MY, Mahmood MR, Aswad MF. Stress distribution from railway track over geogrid reinforced ballast underlain by clay. Earthq Eng Eng Vib. 2019;18(1):77–93.
- [22] Bowles JE. Foundation analysis and design. 5th edn. New York: The McGraw-Hill Companies, Inc; 1996.
- [23] Hoe IL, Ling H, Mohri Y. Parametric studies on the behavior of reinforced soil retaining walls under earthquake loading. J Eng Mech ASCE. 2005;131(10):1056–65.